Applied Energy 109 (2013) 1–9

Contents lists available at SciVerse ScienceDirect

Applied Energy

journal homepage: www.elsevier.com/locate/apenergy

Optimization of thermoelectric topping combined steam turbine cycles for energy economy

Kazuaki Yazawa *, Yee Rui Koh, Ali Shakouri

Birck Nanotechnology Center, Purdue University, United States

HIGHLIGHTS

- Thermoelectric on top of steam turbine cycle provides better energy economy.
- There found an optimum partitioning temperature in between two engines.
- Lower energy cost is found at the max-power at the beginning of operation.
- Higher efficiency operation lowers the energy cost for longer hours.
- Improving *ZT* provides a significant cost reduction for energy production.

ARTICLE INFO

Article history:
Received 27 December 2012
Received in revised form 4 March 2013
Accepted 21 March 2013
Available online 23 April 2013

Keywords:
Thermoelectric
Topping cycle
Steam turbine
Energy economy

ABSTRACT

A mismatch between the fuel combustion temperature ~2250 K (adiabatic) and the high pressure steam temperature up to 900 K, results in a large amount of thermodynamic losses in steam turbine (ST) cycles. A solid-state thermoelectric (TE) placed on top of a ST cycle will produce additional electrical power. By selecting the right materials for the TE generator for high temperature operation, the energy production from the same fuel consumption will increase. Recent nano-structured enhancements to the thermoelectric materials could provide practical performance benefits. We carried out a theoretical study on the optimization of the interface temperature connecting these two idealized engines for energy economy as a combined system. We also analytically studied the optimum point-of-operation between the maximum power output for minimizing the payback and the maximum efficiency to obtain the maximum fuel economy for each generator. The economic optimum ends up in a significant reduction in energy cost ($/kW h). The combined TE topping generator system provides a lower energy cost for any period of operational life and higher interface temperature compared to the ST cycle alone. The maximum power output is observed at around 700 K of interface temperature for 10,000 h of operation, while the minimum energy production cost from the combined system is observed at over 900 K with $ZT = 1$.

1. Introduction

1.1. Energy cost and fuel consumption

A tragedy with a nuclear plant in Fukushima, of Japan raised public concern about nuclear power, not only in Japan but in other countries as well [1]. The national level strategy for power plants may have to consider many additional factors. One of the factors is the energy price ($/kW h). Considering sustainability of oil resources and global warming, without a nuclear approach, we have no choice other than increasing fuel efficiencies or exploring renewable sources such as solar or wind. The US energy flow chart [2] shows that the energy in service is only ~41.7% of the energy input. This study represents one approach for increasing fuel efficiency in power production and lowering the energy cost ($/kW h). Among various power generators, steam turbines, invented by Parsons [3] in 1884, have a long history. This particular mechanism is widely used for power generation. Steam turbines are also one of the most effective mechanical engines [4] due to its relatively simple structure and its intrinsic energy conversion efficiency is closer to the Carnot efficiency. In addition to using saturated steam from a boiler, superheated steam is also used with a compressor for higher efficiency. The thermodynamic conversion efficiency however, is limited by the inlet steam temperature since the structural material of turbines, such as stainless steel, has a temperature-dependent mechanical yield limit at the extremely high steam pressure. For example, the theoretical upper limit thermodynamic efficiency (Carnot efficiency) for a 900 K steam temperature and 300 K ambient temperature is 67%. Furthermore, since the system includes irreversible thermal contacts, we cannot

* Corresponding author.
E-mail address: kyazawa@purdue.edu (K. Yazawa).

0306-2619/$ - see front matter © 2013 Elsevier Ltd. All rights reserved.
http://dx.doi.org/10.1016/j.apenergy.2013.03.050

Nomenclature

d	thickness [m]	U	cost per power [$/W]
m	electrical resistance ratio [–]	Y	energy cost [$/W h]
F	fill factor [–]	w	power per unit area [W/m^2]
I	initial cost [$/W m^2]	β	thermal conductivity [W/mK]
h	life operation hours [h]	η	efficiency [–]
G	unit price [$/kg]	ρ	density [m^3/kg]
q	heat flux [W/m^2]	σ	electrical conductivity [1/Ω m]
S	Seebeck coefficient [V/K]	ψ	thermal resistance [K m^2/W]

obtain any usable power at maximum efficiency. Theoretical efficiency of an ideal thermodynamic engine (with no intrinsic losses) with irreversible contacts is only 42% at the maximum power output based on Curzon and Ahlborn [5]. In this work, we will highlight the validity of adding a thermoelectric (TE) generator on top of a steam turbine (ST) cycle. With an analytical approach, we will find the best operating point for fuel economy for the TE topping ST cycles between the conditions for the maximum efficiency and the efficiency at maximum power output. As an immediate summary, the best achieved efficiencies of other technologies as a function of heat source temperature are given by Vining [6].

1.2. Thermoelectric topping generator on a steam turbine cycle

Here we propose adding a TE power generator into the gap between the flame temperature and the steam temperature. We have studied a combined system composed of a TE generator on top of a ST cycle. The TE generates an additional amount of power by using the large temperature gap between the source temperature and the steam temperature. Even with a special design dedicated for high temperature operation for turbines [7], the steam temperature is limited to <650 °C. Some of the steam turbine cycles work under saturated steam (Rankine cycle). For higher temperature input, recent steam turbines use superheated steam. A Hirn cycle maybe used as a similar cycle using a compressor to obtain a superheated steam under high pressure before boiling, while a Rankine cycle uses a pump to circulate the condensed water back into the boiler. In this work, we simplify the ST cycle as an irreversible engine since the primary interest is on the impact resulting from adding the TE generator on top. Then, we optimize the interfacial temperature for the lowest energy cost.

TE generators have been receiving relatively more attention for the waste heat recovery applications, for which the temperature range is similar to that of saturated steam turbines. There are several studies of TE generators and waste heat recovery systems. Chen et al. [8] reported a comprehensive review of the various applications. Chen et al. [9] studied two stages thermoelectric generators. Caillat et al. [10] studied the graded multiple TE materials for maximizing the practical efficiency of power generation. Qiu and Hayden [11] studied a combined TE and organic Rankine cycles (ORCs) to effectively use the heat exhausted from an organic Rankine cycle turbine with three different modes of TE generators. Gou et al. [12] studied the low-temperature waste heat recovery with TE.

Unfortunately, this solid state device provides only a moderate efficiency despite the research effort spent on the material science. Thus, only the space-limited or weight-limited applications have been heavily investigated, in the area of vehicle exhaust heat recovery [13–15]. However, the solid-state thermoelectric energy conversion is theoretically scalable to temperatures much higher than superheated steam and TE materials are tunable for the targeted temperature. This characteristic becomes an advantage which other technologies could not accommodate. For the higher temperature application of TE generators, several different aspects of concentrated solar TE generators have been studied by Kraemer et al. [16], Yazawa and Shakouri [17], and Xiao et al. [18].

The TE module can be designed for optimum by changing the element thickness to match the external thermal resistances as reported in [19]. Using heat concentration by making the fractional cross section area of the element smaller, orders of magnitude less mass of the material is necessary for the same power output [20] as far as maintaining the thermal resistance match. Earlier we also studied the thermal and electrical parasitic impacts [21] for the optimal design. This optimum TE design takes into account both the initial cost and the operating cost of the fuel.

Knowles and Lee [22] recently studied a combined system placing a TE on top of a Brayton cycle and reported the efficiency at the maximum power output. They pointed out that adding TE only adds the power at the lower temperature range of the turbine but the efficiency cannot exceed that of the high temperature gas turbine. They suggest that using a TE topping cycle is limited to cases for which space or price cannot be justified for a high temperature turbine. To look into the potential for the temperature range, we also extend the calculation to investigate higher interface temperature range.

To evaluate the energy cost of the system, we optimized the design parameters for fuel economy and thus can point out the broader advantages of the TE topping combined system as a function of the operation life time and the fuel cost.

2. Materials and methods

2.1. Model of TE system

The thermal circuit model of the system is shown in Fig. 1. T_g is the interconnecting temperature between the two engines. The power output from the TE is a function of the design parameter d, the thickness of the thermoelement. The parameters are always on a per unit area basis for this analysis.

The external thermal resistances ψ_h and ψ_c (K m^2/W) are assumed to be symmetric. This simplifies the equation since the power output is insensitive to asymmetricity of the thermal contacts. Thus,

$$\psi_h \cong \psi_c \tag{1}$$

$$\frac{(T_h - T_c)}{(T_s - T_g)} = \frac{d}{d + m\beta\sum\psi} = \frac{d}{d + d_0} \tag{2}$$

where d is the element thickness, d_0 is the optimum thickness for the maximum power output. β is thermal conductivity of the TE material and m is a ratio of the electrical load resistance against the internal resistance. T_s is the adiabatic flame temperature of the fuel, T_h and T_c are the hot side and the cold side temperature of the thermoelement, respectively. $\Sigma\psi$ is the sum of the external

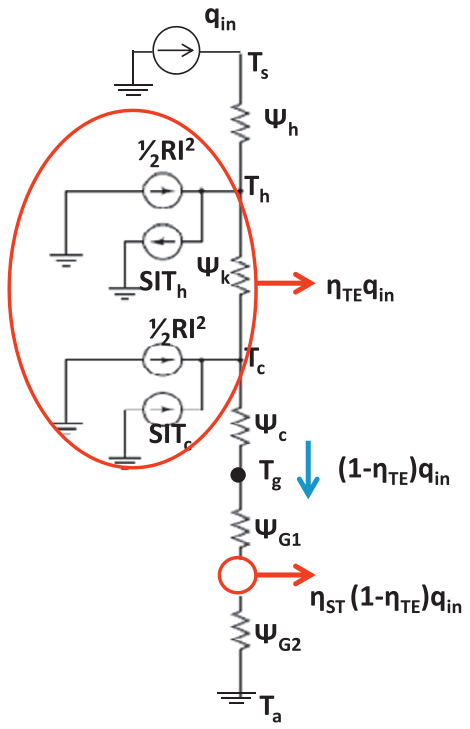

Fig. 1. Thermal network model of the entire system.

thermal resistances thus, $\Sigma\psi = \psi_h + \psi_c$. According to Ref. [19], the optimum is found at,

$$d_0 = m\beta\sum\psi \tag{3}$$

and

$$m = \sqrt{1+Z\overline{T}} \tag{4}$$

where $Z\overline{T}$ is the dimensionless figure-of-merit of the TE material and Z is defined as $Z = \sigma S/\beta$, while σ is electrical conductivity and S is Seebeck coefficient. $\overline{T}$ is the mean operating temperature across the TE element. The generic power output w is found for a given T_h and T_c, as,

$$w_{TE} = \frac{m\beta Z(T_h - T_c)^2}{(1+m)^2 d} \tag{5}$$

The efficiency η_{TE} of the power generation from the thermoelectric device is found as,

$$\eta_{TE} = \frac{w}{q_{in}} = \frac{m\beta Z(T_h - T_c)^2}{(1+m)^2 d}\frac{1}{(T_s - T_h)/\psi_h} \tag{6}$$

where q_{in} is heat flux from the heat source flame.

While $\eta << 1$ considering $ZT \sim 1$, the heat flow through the hot side and the cold side thermal resistances are similar. Thus, $(T_s - T_h)$ and $(T_c - T_g)$ are approximately equal. Based on this, the power output Eq. (5) can be rewritten as,

$$w_{TE} = \frac{Z}{(1+m)^2}\frac{d/d_0}{(d/d_0+1)^2}\frac{1}{\sum\psi}(T_s - T_g)^2 \tag{7}$$

$$\eta_{TE} \cong \frac{Z}{(1+m)^2}\frac{d/d_0}{(d/d_0+1)}(T_s - T_g) \tag{8}$$

Here, power output is found as a function of the dimensionless thickness d/d_0. Other parameters are the given conditions $\Sigma\psi$, T_s, and T_g. Both the extremely thin and thick thermoelement generate nearly zero output according to Eq. (7). This supports the assumption that an optimum exists.

For a specific material, the material properties and Z value are temperature dependent. However, we kept the material properties the same across the temperature range. This is because once the optimum temperature for TE is found, we can chose or develop the material match for the required temperature. Most of the currently available materials show $ZT \sim 1$ for a wide temperature range as seen in the handbook [23]. Despite the fact that ZT is a temperature dependent factor, we keep the properties constant so as to yield $ZT = 1$ at the interface temperature $T_g = 800$ K. The ZT value goes slightly larger for a higher temperature ($T_g > 800$ K) and smaller for the lower ($T_g < 800$ K).

2.2. Energy cost model for TE

Energy cost Y_{TE} ($/kW h) for the thermoelectric section is calculated as follows:

$$Y_{TE} = \frac{I_{TE}}{hw_{TE}} + \frac{Y_f}{\eta_{TE}} \tag{9}$$

where h is the operational life in hours for the design, Y_f is the cost of potential chemical energy of the fuel in units of $/kW h, and I_{TE} ($/m^2) is the initial material cost to build the system per unit area, given by:

$$I_{TE} = \rho dFG + 2\rho_s d_s G_s \tag{10}$$

where subscript s indicates the substrates for the thermoelectric module, ρ is density, F is fill factor, and G is the material market unit price ($/kg). Heat sinks are not included in this part of the model, since they are already included in the Rankine cycle unit. We may replace them with modified versions but do not expect a different price, thus we did not double count the heat sink in Eq. (10).

The first term in Eq. (9) is the payoff for the initial investment. Thus longer term operation yields a smaller energy cost since the initial investment cost is amortized over the number of operating hours. The second term is the operating cost, which is dependent on the fuel cost and the energy conversion efficiency. Therefore, maximizing efficiency or maximizing power impacts each individual term. As Eqs. (7) and (8) show, these factors are tightly related and therefore the relation yields a trade-off.

Substituting Eqs. (7), (8), and (10) into Eq. (9), the energy cost is found as a function of TE leg thickness, d.

$$Y_{TE} = \frac{(\rho dFG + 2\rho_s d_s G_s)(1+m)^2(d/d_0+1)^2}{hZ(d/d_0)(T_s - T_g)^2}\sum_{TE}\psi + \frac{(1+m)^2(d/d_0+1)}{Z(d/d_0)(T_s - T_g)}Y_f \tag{11}$$

For the further simplification, we assume the ratio of the element thickness and the substrate thickness d/d_s is a constant. Considering the mechanical stiffness of the substrate and the necessity of heat spreading in the substrate, it is reasonable to assume a constant relation. Replacing d/d_0 with x, the above equation becomes,

$$Y_{TE} = \frac{(\rho FG + 2\rho_s cG_s)(1+m)^2 d_0(x+1)^2}{hZ(T_s - T_g)^2}\sum_{TE}\psi + \frac{(1+m)^2(x+1)}{Zx(T_s - T_g)}Y_f \tag{12}$$

2.3. Optimization of TE engine

By taking the derivative of Eq. (12), $\frac{\partial}{\partial x}Y_{TE} = 0$, we find the value of x that will minimize Y_{TE}.

The solution is found as Eq. (13) which is the only real formula among the possible three solutions.

$$x = \frac{1}{3}\left(X + \frac{1}{X} - 1\right) \tag{13}$$

while,

$$X = \frac{\sqrt[3]{2}A}{\sqrt[3]{-2A^3 + 27A^2B + 3\sqrt{3}\sqrt{27A^4B^2 - 4A^5B}}} \tag{14}$$

with,

$$A = 2\frac{(\rho FG + 2\rho_s c G_s)(1+m)^2 d_0}{hZ(T_s - T_g)^2}\sum_{\mathrm{TE}}\psi \text{ and } B = \frac{(1+m)^2}{Z(T_s - T_g)}Y_f \tag{15}$$

2.4. Optimization of ST cycle

The steam turbine can be considered with a simpler model, which is comprised of an ideal engine with irreversible thermal contacts for both hot and cold sides. The work generated by the turbine is considered as electrical power. The efficiency of the steam turbine cycle η'_{ST} includes all of the mechanical energy transfer efficiency ~65% combining the turbine and the compressor/pump and the mechanical-to-electrical conversion efficiency ~92% out of the thermodynamic efficiency η_{ST}. If the cycle is ideally flexible for the "design to the target", the efficiency is considered as the $\eta_{ST} = 1 - T_a/T_g$ for the reversible core of the engine with a coefficient C_{ST}. Thus the efficiency of the ST cycle containing irreversible contacts becomes $\eta'_{\mathrm{ST}}/C_{\mathrm{ST}} = \eta_{\mathrm{ST}}$.

$$Y_{\mathrm{ST}} = \frac{I_{\mathrm{ST}}}{hw_{\mathrm{ST}}} + \frac{Y_f}{C_{\mathrm{ST}}\eta_{\mathrm{ST}}} \tag{16}$$

From the conservation of energy and the conservation of entropy, the relation of the power output and the efficiency is described as,

$$w_{\mathrm{ST}} = \frac{1}{\sum_{\mathrm{ST}}\psi}\frac{\eta'_{\mathrm{ST}}/C_{\mathrm{ST}}(T_g - T_a - T_g\eta'_{\mathrm{ST}}/C_{\mathrm{ST}})}{1 - \eta'_{\mathrm{ST}}/C_{\mathrm{ST}}} \tag{17}$$

The initial cost I_{ST} is considered to build the system for maximum power. By following Curzon–Ahlborn maximum power is given by the contact temperatures T_g and T_a.

$$I_{\mathrm{ST}} = U_{\mathrm{ST}}w_{\mathrm{ST\_max}} = U_{\mathrm{ST}}\frac{1}{\sum_{\mathrm{ST}}\psi}\left(T_g - 2\sqrt{T_aT_g} + T_a\right) \tag{18}$$

where, $\sum_{ST}\psi$ is the sum of the irreversible thermal resistance per unit area (K m^2/W) within the steam turbine. Substituting Eqs. (17) and (18) into Eq. (16),

$$Y_{\mathrm{ST}} = E\frac{(A - \eta'_{\mathrm{ST}})}{(B - C\eta'_{\mathrm{ST}})\eta'_{\mathrm{ST}}} + \frac{D}{\eta'_{\mathrm{ST}}} \tag{19}$$

where,

$$A = C_{\mathrm{ST}}, B = (T_g - T_a)C_{\mathrm{ST}}, C = T_g, D = Y_f, E = \frac{Y_i}{h}\left(T_g - 2\sqrt{T_aT_g} + T_a\right)C_{\mathrm{ST}} \tag{20}$$

Similar to the thermoelectric engine, we find the efficiency. The solution is found as,

$$\eta'_{\mathrm{ST}} = \frac{(AE + BD) - \sqrt{(AE + BD)^2 - B(CD + E)(AE + BD)/C}}{(CD + E)} \tag{21}$$

Due to the model simplification, the components not considered here are (1) the efficiency degradation through the auxiliary components, e.g. pressure losses of working fluid, (2) temperature dependency of thermal properties of the working fluid, and (3) non-linear mechanical losses of turbines and generators. However, in this analysis, the impact of interfacial temperature is the primary interest and the difference between a single ST and the TE combined system. To evaluate the differences, using the theoretical upper limit of ST could be reasonable to measure the validity of adding TE. Instead of considering a particular system, this model provides seamless scalability for the interfacial temperature.

2.5. Nanostructured TE materials

Returning to the TE generator, it is not obvious from Eq. (12) but careful investigation reveals that a material with a larger figure-of-merit could provide a lower energy cost. The infinitely large ZT gives $Y_{\mathrm{TE}} \to Y_{\mathrm{TE\_ZT=1}}/(3 + 2\sqrt{2})$ at the maximum power output, while the load resistance ratio $m = \sqrt{1 + ZT}$. Thus, improving the material figure-of-merit (ZT value) is an important technological development. As reported in [20], the thermal conductivity is the most influential parameter for the lower mass use of these expensive materials.

Shakouri [24] provided a comprehensive summary of recent developments. Due to the nature of thermoelectric properties, it is quite difficult to find a natural material which has a very large ZT. Similar to high speed electronic applications where electrical properties of semiconductors are engineered, thermoelectric materials are also engineered by manipulating the atomic scale characteristics. It is well known that the thermal conductivity of semiconductors consists of two components. One is lattice thermal conductivity which is due to the phonon heat transport and the other is electronic thermal conductivity. The latter is constrained to electrical conductivity by the Weidman–Franz law. Phonon scattering approach [25] to reduce the lattice thermal conductivity is performed by superlattices, embedded nanoparticles and rough nanowire structures. Some semiconductors are available to work at high temperature such as Si/SiGe used in radioisotope thermoelectric generators with a maximum ZT at 900 K or higher [23]. Boron compounds can work at 1300–1500 K [23]. This is one of the advantages of solid-state thermoelectric devices for applications similar to this study.

2.6. Conditions and parameters for analysis

Material properties of thermoelement:

Base line thermoelectric properties, the figure-of-merit ZT becomes approximately 1.

Thermal conductivity β = 1.5 (W/m K)
Electrical conductivity σ = 25,000 (1/Ω m)
Seebeck coefficient $S = 2 \times 10^{-4}$ (V/K)
Density ρ = 8200 (kg/m^3)

Cost factors:

TE material price 500 ($/kg)
Steam turbine system machine cost (overnight cost) 7000 ($/kW)
Fuel cost 0.108 ($/kW h)

The machine cost of the bottoming cycle is difficult to find. Additionally, also the cost per unit power depends on the scale. We only found the unit cost of a micro-gas turbine [26]. Since we are interested in different interface temperatures, the extrinsic mechanisms such as heat exchangers may have similar costs. The fuel cost is calculated based solely on the market prices of gasoline and natural gas as well as the calorific value of the fuels. The

calorific value comes from [27]. To make the cost impact clear, the auxiliary costs or interposed cost are not considered for the calculation. Interestingly the price for calorific value was quite similar for gasoline and liquid propane gas (LPG). This cost value is also the bottom line for the electricity supply cost. As far as relying on burning a fuel, the electricity cost cannot be lower than the value, 0.108$/KW h based on the fuel price.

Performance factors:

Thermal resistances ψ_h and ψ_c are 0.005 (K m^2/W) each.
Thermal resistances in steam turbine (heat sinks) $\psi_{G1} = \psi_{G2}$: pseudo defined (K m^2/W)

Temperatures: the flame T_s = 2250 (K) and the ambient T_a = 300 (K)

ST generator's performance constant C_{ST} is assumed to be 65% × 92% = 60%. The mechanical efficiency is in a similar range as the efficiency used in Ref. [22] for Brayton cycle turbines.

The adiabatic flame temperature is from [28]. Another parameter, Fill factor = 10% (fractional area coverage of TE element relative to the cross section area of the heat flow). With this range the substrate cost is in a range of 10%, so that the following calculations neglect the cost of the TE substrate.

The analysis is carried out as a function of the operational life in hours for each design h and the interface temperature T_g.

3. Results and discussion

3.1. Thermoelectric generator part

Fig. 2a shows the power output and the heat flux per unit cross-section-area of heat flow and Fig. 2b shows the energy conversion efficiency. Both are functions of the dimensionless leg thickness, d/d_0. The maximum power output at time = 0 is found at $d = d_0$. A thicker TE element leads to a larger efficiency but it significantly limits the heat flow, thus the power output decreases as the element becomes thicker. We analytically showed this behavior in Ref. [19].

Fig. 3 shows the dimensionless thickness d/d_0 optimized for the lowest energy cost and energy conversion efficiency, both as the functions of the operation hours. Over 2000 h, the optimum thickness is larger than that of the maximum power output. This is due to better fuel efficiency. As the operation hours become longer, the econo-optimum design approaches to the maximum efficiency.

3.2. Steam turbine part

The following Figs. 4–6 are based on 800 K for the interface temperature. Fig. 4 shows the energy cost as a function of efficiency for variations of operation hours. For a small amount of hours, the energy cost is dominated by the payback for the initial cost of the generator. For longer operation, the energy cost drop gradually. The efficiency at minimum energy cost depends on the operating hours. This cost-minimum efficiency is found to be lower for longer operational life. Finally, for very long operating hours, the energy cost continues to drop as the efficiency increases. The relationship between the power output and the efficiency of the idealized thermodynamic cycle is shown in Fig. 5. Any thermodynamic system which has irreversible thermal contacts exhibits similar behavior. Considering that we have the freedom to change the internal thermal resistance starting from zero, the power output increases as increasing the resistance by increasing temperature difference across the generator. At some point, the power output will reach the maximum and then decrease while efficiency increases since the temperature difference is still increasing. Finally, the infinitely large internal resistance yields the maximum efficiency, but the power goes to zero since the heat can no longer be transferred. In this analysis, we applied a constant factor C_{ST} to model the intrinsic thermodynamic performance to the Carnot cycle, which is shown on the curve with maximum efficiency of 23.3%. Fig. 6 shows the econo-optimum efficiency as a function of the operation hours. Similar to the TE analysis in Fig. 3, the optimum operating efficiency is always higher for a longer period of operation and it converges to the maximum efficiency for an infinitely long period of operation.

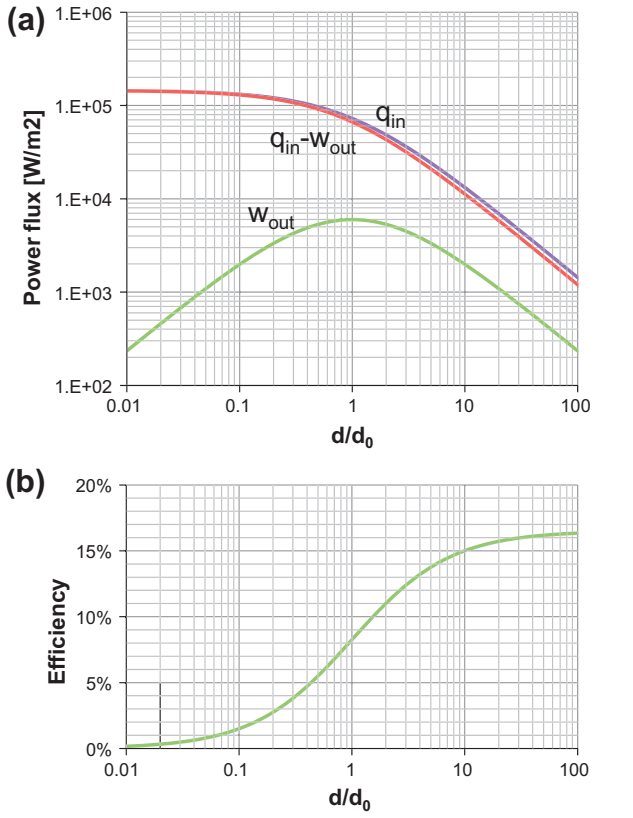

Fig. 2. (a) Power output and heat flow per unit area and (b) energy conversion efficiency as a function of the dimensionless leg thickness.

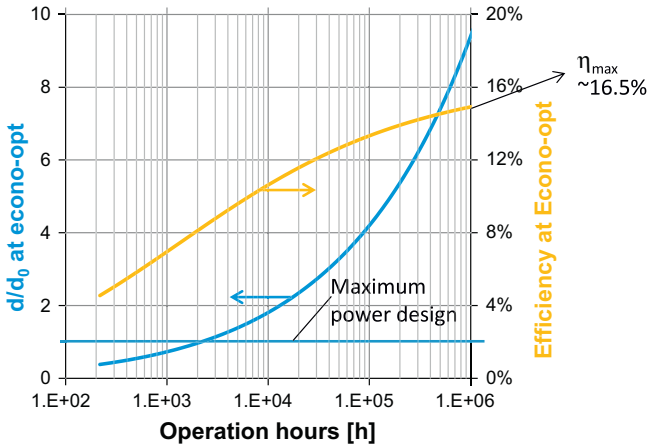

Fig. 3. The optimum d/d_0 and its efficiency vs. hours of operation.

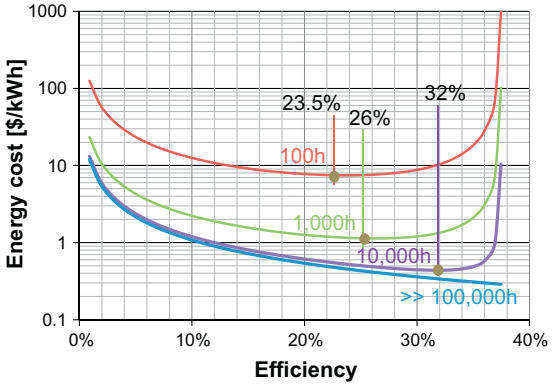

Fig. 4. Energy cost vs. operating efficiency for Rankine cycle. T_g = 800 K.

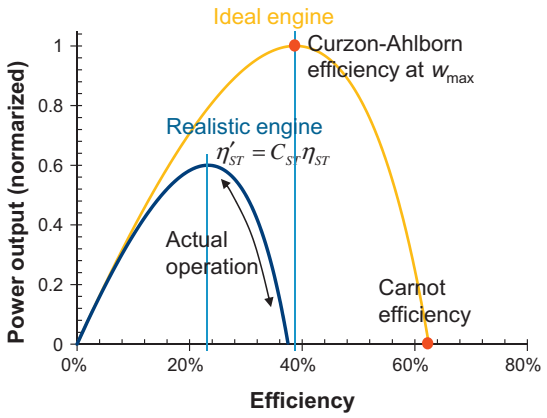

Fig. 5. Power output vs. operating efficiency at T_g = 800 K while T_a = 300 K. The shrunk curve includes the efficiency coefficient C_{ST} = 60% relative to Carnot engine. The economic optimum is found in between the conditions of the maximum power output and the maximum efficiency.

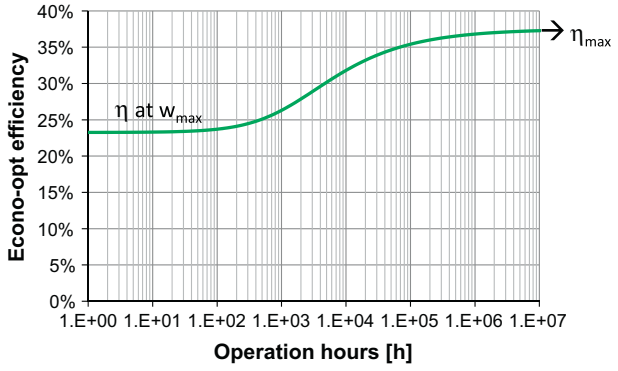

Fig. 6. Efficiency at economic optimum condition vs. the life operation hours.

3.3. Power output of the combined system

Fig. 7a and b shows the econo-optimum power output for the TE part, ST part, and the combined system. A dotted curve shows the econo-optimum ST alone if there was no upper temperature limit. Fig. 7a shows that the combined system generates more power compare to the bottoming cycle (ST) alone from the same heat source. The output power tends to decrease due to the econo-optimum shift to the design for efficiency at longer life operation. We observe a peak for TE at around 1000 h. Fig. 7b shows the impact of the interface temperature T_g on power output at an

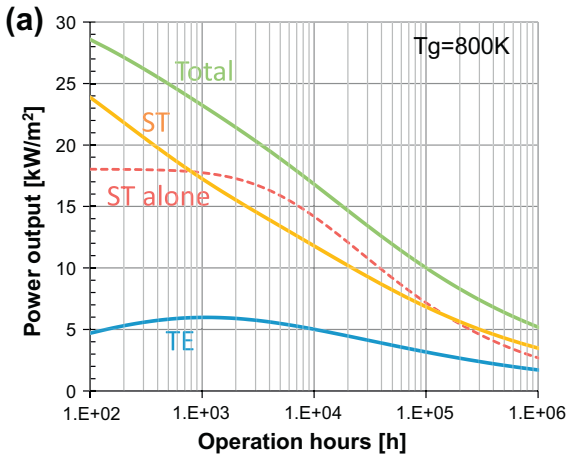

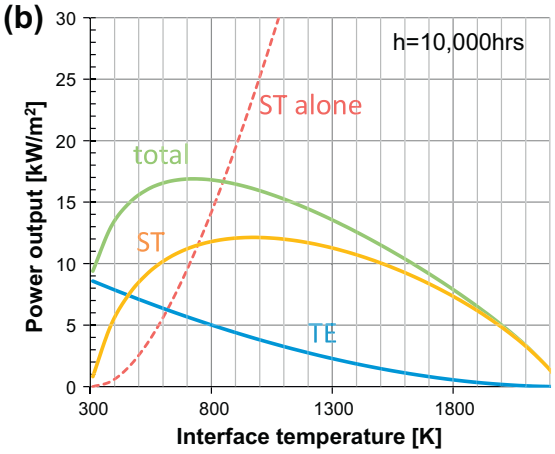

Fig. 7. Economical optimum power output for the lowest energy cost as (a) functions of operation hours and (b) interface temperature. (a) Is a plot for 800 K of the interface temperature and (b) is a plot for 10,000 h of operation. 'ST only' points the steam turbine only white 'TE' and 'ST' indicate the TE generator and the ST cycle components of the combined system. *ZT* is approximately 1.

operation life of 10,000 h. We observe an optimum T_g for maximum power output at around 700 K. The temperature at which the power output peaks for the combined system is lower than that for the bottoming cycle (~1100 K). This is due to the continuously decreasing output from TE as the interface temperature increases.

3.4. Efficiency of the combined system

Fig. 8a and b shows the efficiency calculated for the same systems as above. For the design for longer operation hours, both TE and ST converge to the maximum efficiency for each individual systems.

Fig. 8b also includes the impact of enhancing the material *ZT* factor (*ZT* = 1, 2, and 5) by changing thermal conductivity. The *ZT* = 2 curve corresponds to a range of advanced high-end materials ever fabricated and characterized [23] whereas *ZT* = 5 suggests the future desire for TE materials. At *ZT* = 5 values stand alone thermoelectric could provide similar performance to a practical vapor compression cycle in refrigeration. In the combined system, TE provides a minor improvement in efficiency, but plays a relatively significant role at lower interface temperature. Ref. [6] provided the best practice efficiencies for Nuclear Brayton cycle + Rankine cycle. Unfortunately, based on our analysis, the theoretical combined system of TE (*ZT* = 1) on top of Rankine cycle could not achieve the best ever marked efficiency (~50%) for the same source temperature. The engineering of TE materials with *ZT* = 4–5 may be

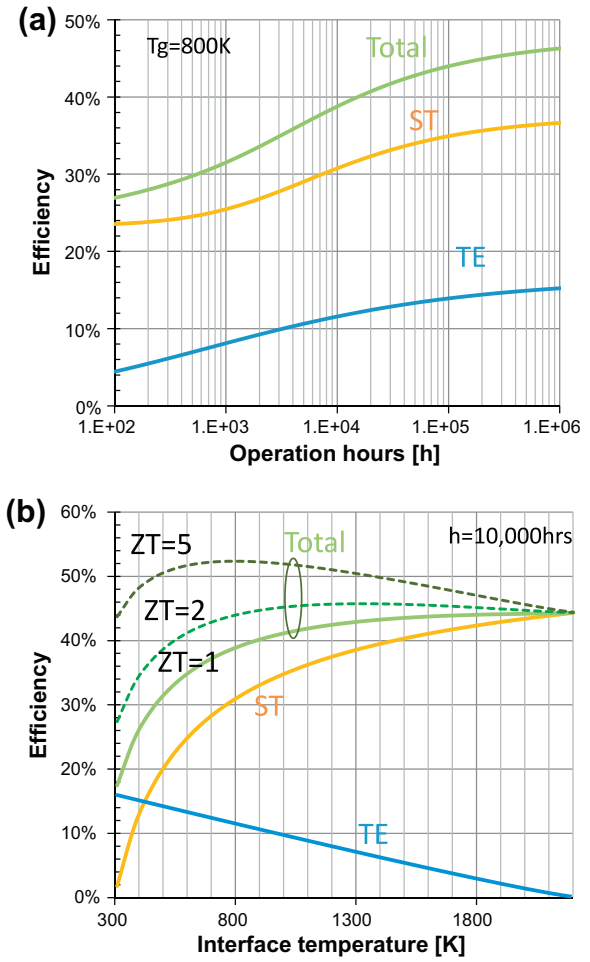

Fig. 8. Efficiency as a function of (a) operation hours and (b) interface temperature. (a) Is a plot for an interface temperature of 800 K and (b) is a plot for 10,000 h of operation with approximately $ZT = 1$ and dashed curves shows the case of approximately $ZT = 2$ and $ZT = 5$.

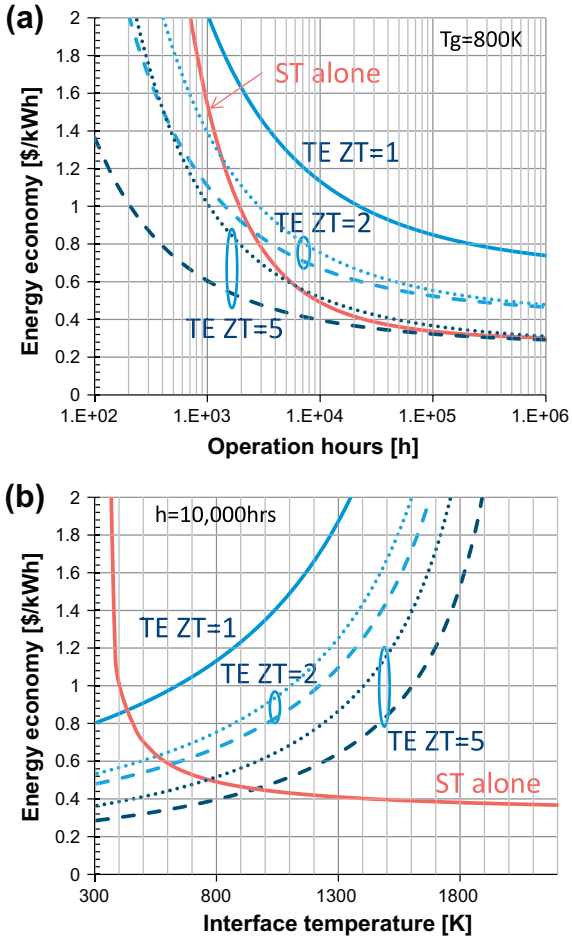

Fig. 9. Energy cost of steam turbine only and TE only vs. (a) operation hours and (b) interface temperature. (a) Is a plot for an interface temperature of 800 K and (b) is a plot for 10,000 h of operation, with variation of the material properties of TE ($ZT = 1$, 2, and 5). Dotted curves show the impact of improving power factor and dashed curves show the impact of thermal conductivity.

necessary to reach the best efficiency. Similar to the single cycle efficiency of Coal Rankine cycle, Solar Brayton cycle efficiency is also found to be ~50%. Nevertheless, there is still a room to put TE on top of them to enhance the efficiency.

3.5. Energy economy analysis

The energy production cost ($/kW h) of TE part of the system is plotted in Fig. 9 compared to the standalone ST. A variation of the thermoelectric properties are also considered ($ZT = 1$, 2, and 5). The trends for operation hours in Fig. 9a shows a similar trend for each scenario, but the trend for interface temperature in Fig. 9b shows the trade-off behavior between the TE and ST. The impact of enhancing the Z factor ($Z = \sigma S^2/\beta$) is separated by the change in power factor (σS^2) indicated by dotted curves, and the change in thermal conductivity (β) indicated by dashed curves. The difference is smaller for longer operating period and the energy cost of $ZT = 5$ is projected to be comparable to ST. Fig. 10 shows the total energy production cost of the combined system in comparison to the standalone ST. As seen in Fig. 10a, longer life operation always lowers the energy cost. Cost reduction contribution of the TE topping cycle is approximately 20% of the combined system at infinitely long operation hours. The interface temperature dependency is shown in Fig. 10b. There is a very flat valley for the energy cost between 800–1200 K interface temperature with $ZT = 1$. However, this characteristic shifts to a lower cost at a lower interface temperature with more advanced TE material. Looking at the other technologies, the market price of electricity, which is very low around 0.1 $/kW h in the United States, is the only reasonable way to compare. In this case, the Rankine cycle even with TE topping cycle may not be the first option for electricity production and may need an additional consideration for the by-product of heat (e.g. co-generation applications).

3.6. Practical limitation of the systems

The optimum temperature (~700 K) to achieve the peak power output in Fig. 7b is preferable to considering a practical machine for the bottoming cycle since the source temperature is limited by some structural materials as well as the pressure limit of the superheated steam. For the lower temperature side, the steam might be saturated steam or the steam may be replaced by an organic working fluid. Under 500 K, total efficiency is already so low it may not pay to find the optimum temperature but TE does play a major role at the lower temperatures. It is fortunate that the peak efficiency of the combined system shows a plateau-like curve, thus the optimum design is quite robust.

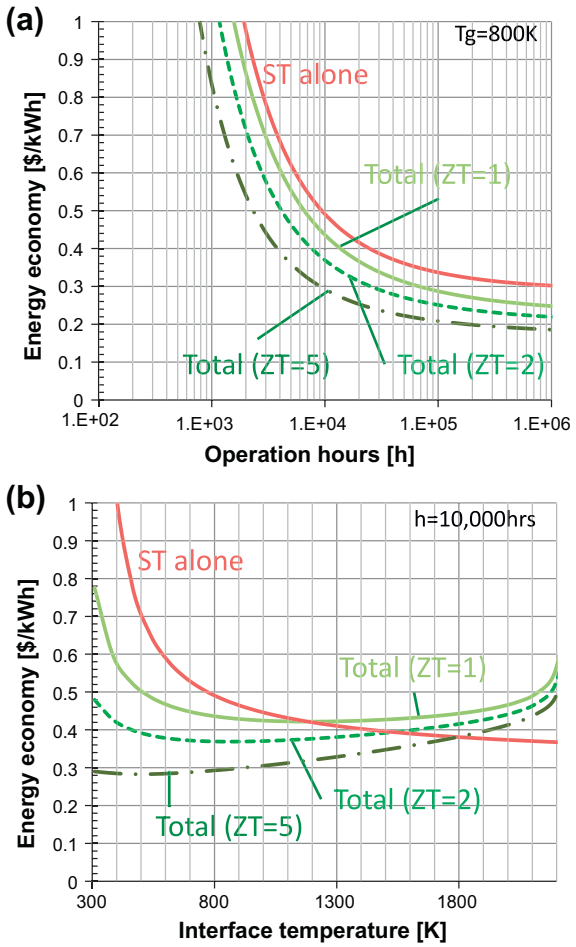

Fig. 10. Energy total energy cost in comparison to the steam turbine only vs. (a) Operation hours and (b) interface temperature, with variation of *ZT* of TE (*ZT* = 1, 2, and 5).

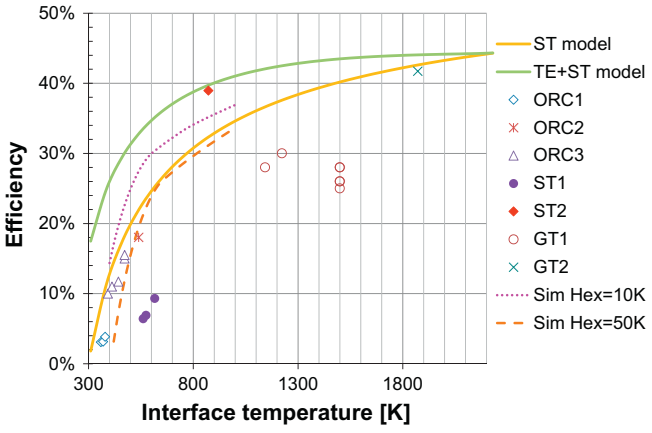

Fig. 11. Comparison of efficiency for a variety of turbine generators to the model. The achieved data refers ORC1: Ref. [29], ORC2: Ref. [30], ORC3: Ref. [31], ST1: Ref. [32], ST2: Ref. [33], GT1: Ref. [34], GT2: Ref. [35], respectively. Also, numerical simulation results indicated by two dashed curves are plotted.

3.7. System scale for applications

The thermoelectric generator is scalable since it can be designed in an array. Practically, we may have to wait for mass production to mature. A lower temperature range with moderate scale ranging 10s kW – a few MW of ORCs or STs would be an advantageous area for the TE topping system in terms of energy cost. In contrast a technology like a nuclear plant, which is a few GW in scale, cannot be scaled to a few MW range. For the temperature scaling, even with a state-of-the-art material applied, reaching the gas temperature of 1200 K is not easy for Brayton cycles. For the TE materials, there is already some options as stated in Section 2.5.

3.8. Efficiency reported for real systems compared to simulations

The achieved efficiencies from data reported in the literature vs. inlet temperature are shown in Fig. 11. We also plot the simulation results based on the Rankine cycle process referring to the *T*–*S* diagram of water–vapor for two cases of heat exchanger designs. 10 K and 50 K indicates the temperature difference across the hot side and the cold side heat exchangers. Note that the ORCs performance and temperature range differ depending on the working fluid. Among the data points, ST2 shows an irregularly high efficiency compared to the others. The data points do not necessarily match since the goal of our model is to obtain the minimum energy cost. The model is however, a reasonable fit in the practical range. This graph also shows the benefit of adding TE.

4. Conclusions

We developed a generic model and analyzed energy economy for a combined TE generator on top of a steam turbine cycle. The optimum design/operation for the lowest energy cost both for TE and ST are analytically found. The advantage of adding a TE on top of a ST is demonstrated. The optimum design and the optimum operation of each engine minimize the payback of the initial cost per unit power output. It also simultaneously minimizes the fuel consumption per unit power output. The optimum balance of the design/operation point between the maximum power and the maximum efficiency depends on the hours of operation. Another factor for optimizing the system is the interface temperature between the two engines. A higher interface temperature lowers the energy cost, but there is a practical temperature limitation. The improved thermoelectric figure-of-merit (*ZT*), via e.g. nanostructured material is a key to the successful increase in power output and significant reduction in fuel consumption. We also pointed out the impact of the TE properties for power generation.

Overall, the analysis demonstrated the best balance between lowest fuel consumption and maximum power density. By adding TE on top of the ST cycle, the energy economy increases by effectively reusing a large amount of collateral heat losses that would otherwise occur within a standalone ST cycle.

Acknowledgements

This study was supported by the Center of Energy Efficient Materials, one of the Energy Frontier Research Centers (EFRC) of The Office of Science, US Department of Energy. Authors thank to Dr. Braun and Mr. James for their help on the Rankine cycle simulation.

References

[1] New York Times on-line topic, Nuclear Energy, October 12, 2012. <http://topics.nytimes.com/top/news/business/energy-environment/atomic-energy/index.html>.
[2] Lawrence Livermore National Laboratory, Energy flow chart – Estimated Energy Use in 2011: 97.3 Quads, 2012. <http://flowcharts.llnl.gov/>.
[3] Parsons Charles A. The steam turbine. Cambridge University Press; 1911.
[4] Wiser WH. Energy resources. Springer; 2000.
[5] Curzon F, Ahlborn B. Efficiency of a Carnot engine at maximum power output. Am J Phys 1975;43(1):22.

[6] Vining CB. An inconvenient truth about thermoelectrics. Nat Mater 2009;8:83–5.
[7] Imano S, Saito E, Iwasaki J, Kitamura M. High-temperature steam turbine power plant. US Patent Application 20080250790.
[8] Chen M, Lund H, Rosendahl LA, Condra TJ. Energy efficiency analysis and impact evaluation of the application of thermoelectric power cycle to today's CHP systems. Appl Energy 2010;87(4):1231–8. http://dx.doi.org/10.1016/j.apenergy.2009.06.009. ISSN 0306-2619.
[9] Chen L, Li J, Sun F, Wu C. Performance optimization of a two-stage semiconductor thermoelectric-generator. Appl Energy 2005;82(4):300–12. http://dx.doi.org/10.1016/j.apenergy.2004.12.003. ISSN 0306-2619.
[10] Caillat T, Fleurial J-P, Snyder GJ, Borshchevsky A. Development of high efficiency segmented thermoelectric unicouples. In: Proceedings of ICT2001; 2001. p. 282–5.
[11] Qiu K, Hayden ACS. Integrated thermoelectric and organic Rankine cycles for micro-CHP systems. Appl Energy 2012;97:667–72. http://dx.doi.org/10.1016/j.apenergy.2011.12.072. ISSN 0306-2619.
[12] Gou X, Xiao H, Yang S. Modeling, experimental study and optimization on low-temperature waste heat thermoelectric generator system. Appl Energy 2010;87(10):3131–6. http://dx.doi.org/10.1016/j.apenergy.2010.02.013. ISSN 0306-2619.
[13] Fairbanks JW. Vehicular thermoelectrics: a new green technology. In: Proceedings of the 2nd thermoelectrics applications, workshop; 2011.
[14] Hussain QE, Brigham DR, Maranville CW. Thermoelectric exhaust heat recovery for hybrid vehicles. SAE Int J Eng 2009;2(1):1132–42.
[15] LaGrandeura1 JW, Bella1 LE, Crane DT. Recent progress in thermoelectric power generation systems for commercial applications. MRS Proc 2011;1325.
[16] Kraemer D, Poudel B, Feng H-P, Caylor JC, Yu B, Yan X, et al. High-performance flat-panel solar thermoelectric generators with high thermal concentration. Nat Mater 2011;10:532–8. http://dx.doi.org/10.1038/nmat3013.
[17] Yazawa K, Shakouri A. System optimiztion of hot water concentrated solar thermoelectric generation. In: Proceedings of the 3rd international conference on thermal issues in emerging technologies theory and applications (ThETA3); 2010. P. 283–90.
[18] Xiao J, Yang T, Li P, Zhai P, Zhang Q. Thermal design and management for performance optimization of solar thermoelectric generator. Appl Energy 2012;93:33–8. http://dx.doi.org/10.1016/j.apenergy.2011.06.006 [ISSN 0306-2619].
[19] Yazawa K, Shakouri A. Optimization of power and efficiency of thermoelectric devices with asymmetric thermal contacts. J Appl Phys 2012;111(2):024509. 6 pages.
[20] Yazawa K, Shakouri A. Optimizing cost-efficiency trade-offs in the design of thermoelectric power generators. Environ Sci Technol – J Am Chem Soc 2011;45(17):7548–53.
[21] Yazawa K, Shakouri A. Cost-effective waste heat recovery using thermoelectric systems. Invited Feature Paper, Journal of Material Research 2012; 27:1–6.
[22] Knowles CB, Lee H. Optimized working conditions for a thermoelectric generator as a topping cycle for gas turbine. J Appl Phys 2012;112:07351. http://dx.doi.org/10.1063/1.4757008. 8 pages.
[23] Rowe DM, editor. Thermoelectric handbook macro to nano. CRC Press; 2006.
[24] Shakouri A. Recent developments in semiconductor thermoelectric physics and materials. Annu Rev Mater Res 2011;41:399–431.
[25] D. L. Nika, E. P. Pokatilov, A. A. Balandin, V. M. Fomin, A. Rastelli, and O. G. Schmidt Reduction of lattice thermal conductivity in one-dimensional quantum-dot superlattices due to phonon filtering, Physical Review B, Vol. 84, 165415, (7 pages), (2011).
[26] You-hong Y, Feng-rui S. Thermoeconomics cost modeling of marine gas turbine generating unit. Proceedings of industrial engineering and engineering management (IEEM), IEEE; 2010. p. 2004–8.
[27] Bauer H, editor. Automotive handbook. Robert Bosch GmbH; 1996. p. 238–9.
[28] van Maaren A, Thung DS, de Goey LRH. Measurement of flame temperature and adiabatic burning velocity of methane/air Mixtures. Combust Sci Technol 1994;96(4–6):327–44.
[29] Tahir MbM, Yamada N, Hoshino T. Efficiency of compact organic Rankine cycle system with rotary-vane-type expander for low-temperature waste heat recovery. Int J Civil Environ Eng 2010;2(1):11–6.
[30] Turboden Heat Recovery Unit. <http://www.turboden.eu/en/products/products-hr.php>.
[31] Yamada N, Mohamad MNA, Kien TT. Study on thermal efficiency of low- to medium-temperature organic Rankine cycles using HFO-1234yf. Renew Energy 2012;41:368–75. http://dx.doi.org/10.1016/j.renene.2011.11.028.
[32] Energy and Environmental Analysis, Technology Characterization: Steam Turbines, Report prepared for US Environmental Protection Agency; 2008. p. 13.
[33] GE D-17 Steam Turbine. <http://www.ge-flexibility.com/products-and-services/steam-turbines/d17-steam-turbine.html>.
[34] D. Thimsen, Assessment of Leading Microturbine Technologies: EPRI, 1004454; 2003.
[35] Mitsubishi Power Systems M501 J series. <http://www.mpshq.com/products/gas_turbines/index.html>.